J. Fluid Mech. (2006), *vol.* 565, *pp.* 461–475. © 2006 Cambridge University Press
doi:10.1017/S0022112006001947 Printed in the United Kingdom

On the Rayleigh–Bénard problem: dominant compressibility effects

By A. MANELA† AND I. FRANKEL

Faculty of Aerospace Engineering, Technion-Israel Institute of Technology, Haifa 32000, Israel

(Received 26 September 2005 and in revised form 12 May 2006)

We study the linear temporal hydrodynamic stability in the Rayleigh–Bénard problem for a compressible fluid (a perfect gas) under marginally super-adiabatic conditions, i.e. when the ambient temperature gradient only slightly exceeds the adiabatic gradient and then only within the fluid adjacent to the upper (cold) wall. The onset of convection in this limit demonstrates some unique features which differ qualitatively from those of the familiar Boussinesq approximation. Thus, the ensuing convection is effectively confined to a narrow domain of the fluid close to the upper wall and is characterized by large wavenumbers. Furthermore, these distinct attributes persist with diminishing temperature difference, implying that the prevailing generalized Boussinesq approximation (based on the use of the potential temperature gradient) is non-uniform in the present limit. This non-uniformity is resolved in terms of the small yet significant variations of fluid properties (which are commonly neglected). We comment on the analogy between the present problem and the Taylor–Couette problem for a viscous incompressible fluid within a narrow gap between counter-rotating cylinders. We briefly discuss the potential relevance of the present limit to some recent observations of the onset of convection within near-critical fluids.

1. Introduction

The onset of Rayleigh–Bénard (RB) convection in a fluid confined between horizontal planes and heated from below is a classical problem in hydrodynamic stability theory and has accordingly been studied extensively (Chandrasekhar 1961; Koschmieder 1993). Most of these analyses have been carried out within the framework of the Boussinesq approximation, i.e. the fluid is regarded as essentially incompressible and possessing constant properties (e.g. viscosity and thermal conductivity). Only density variations resulting from thermal expansion are accounted for and then only in the buoyancy term of the equation of motion. The stability problem thus obtained is governed by a single parameter, the Rayleigh number (Ra), representing the relative effects of buoyancy, fluid viscosity and heat conductivity. Transition to convection thus takes place when a critical value $Ra = Ra_{cr}(\approx 1708)$ is exceeded and is characterized by a critical dimensionless wavenumber (normalized by D, the gap width) $k = k_{cr}(\approx 3.117$, both values for infinite planar walls). Provided that compressibility effects (i.e. density variations brought about by pressure gradients) are negligible, the Boussinesq approximation may be substantiated in the limit of small temperature differences (Tritton 1988).

† Present address: Department of Mathematics, Massachusetts Institute of Technology, Cambridge MA 02139, USA.

Most of the analyses which have hitherto addressed the RB problem for a compressible fluid have relaxed either one but not both of the above restrictions. Thus, Paolucci & Chenoweth (1987) and Frölich, Laure & Peyret (1992) studied the effects of substantial temperature variations across the layer while retaining the assumption that pressure- and hence compressibility-induced density variations across the fluid were negligible. According to these studies the onset of convection is still governed by a critical value of Ra. However, owing to the variation of the transport coefficients with the local gas temperature, the pertinent critical value is growing substantially with increasing temperature differences.

When considering compressibility effects, it is necessary for the onset of convection that the adiabatic expansion of a fluid element rising through the hydrostatic pressure field has its density reduced below the ambient reference value. This is usually expressed as a condition on the vertical temperature gradient requiring that it be smaller than the adiabatic gradient corresponding to the ambient hydrostatic pressure distribution, i.e. (Landau & Lifshitz 1959)

$$\frac{\mathrm{d}T}{\mathrm{d}y} < -\frac{\alpha T g}{c_p}, \tag{1.1}$$

wherein T denotes the absolute temperature, y is a Cartesian coordinate in the vertical (upward) direction, α is the coefficient of thermal expansion, g is the gravitational acceleration and c_p the specific heat at constant pressure. In natural situations (e.g. on atmospheric scales) the Rayleigh criterion is trivially satisfied. Transition to convection is thus usually governed by (1.1) (Tritton 1988).

Compressibility effects have been studied, among others, by Jeffreys (1930), Spiegel (1965), Giterman & Shteinberg (1970) and more recently Bormann (2001). They have considered small temperature variations and hence assumed uniform fluid properties and temperature gradient across the fluid layer. Under these conditions the Boussinesq approximation remains valid provided that the actual gradient is replaced by the potential temperature gradient (namely, the excess of the actual over the adiabatic temperature gradient).

The RB problem for arbitrary temperature differences and compressibility effects has in recent years been addressed for rarefied gases in the continuum limit of small Knudsen (Kn) numbers. Most of these studies make use of a molecular approach to simulate the time evolution of the system response by means of the direct simulation Monte Carlo (DSMC) method (Stefanov & Cercignani 1992; Golshtein & Elperin 1996; Stefanov, Roussinov & Cercignani 2002) or finite difference computation based on the Bhatnagar–Gross–Krook (BGK) model equation (Sone, Aoki & Sugimoto 1997). Recently, Manela & Frankel (2005*a*) have carried out a linear temporal stability analysis of a compressible continuum slip-flow model. This linear analysis obtains the neutral curve marking transition to convection in the Froude–Knudsen plane of parameters in agreement with the results of Stefanov *et al.* (2002). According to both calculations, for sufficiently small $Kn > 0$ the convection domain is confined to some finite interval of Froude (Fr) numbers. By definition (for a perfect gas) $Fr = 2RT_h/gD$ (wherein R is the gas constant and T_h denotes the absolute temperature of the lower (hot) wall) describes the relative magnitude of thermal and gravitational effects. At large values of Fr the latter effect is small, the pressure becomes nearly uniform across the fluid layer (see (2.8)) and compressibility effects become negligible. The neutral curve accordingly approaches a curve of constant Rayleigh number which, owing to large temperature differences, is larger than the above Boussinesq critical value (cf. Frölich *et al.* 1992).

With decreasing Froude number, compressibility effects associated with the hydrostatic pressure distribution become increasingly important in determining the density

distribution. Eventually, for sufficiently small Kn, (1.1) determines the actual lower bound on Fr (see (1.2) *et seq.*) and thereby the location of the neutral curve (rather than merely imposing a necessary condition). We use the term 'dominant compressibility' to designate this situation. The results of Stefanov *et al.* (2002) and Manela & Frankel (2005*a*) demonstrate that the onset of convection under these conditions is characterized by some unique features: the ensuing convection is effectively concentrated in a narrow domain adjacent to the upper (cold) wall and the corresponding critical wavenumbers are much larger in comparison with the familiar value resulting from the Boussinesq approximation. Furthermore, Manela & Frankel (2005*b*) confirm that these phenomena persist for all (however small) temperature differences. This appears at variance with the common view (e.g. Tritton 1988) regarding the validity of the above-mentioned generalized Boussinesq approximation based on the potential temperature gradient (see § 4). The main thrust of the present contribution is thus to resolve the transition to convection under dominant compressibility effects.

As a preliminary toward this end we examine how (1.1) is satisfied for a non-constant thermal conductivity. Normalizing the temperature by T_h and the vertical coordinate by D, we write (1.1) for a perfect monatomic gas

$$Fr > -\frac{4}{5}\left(\frac{\mathrm{d}T^{(0)}}{\mathrm{d}y}\right)^{-1}. \tag{1.2}$$

wherein $T^{(0)}(y)$ denotes the dimensionless temperature distribution (e.g. (2.8)) in the reference, pure-conduction state. For a thermal conductivity $\kappa(T)$ which is an arbitrary monotonically increasing function of T, $\mathrm{d}T/\mathrm{d}y(<0)$ is monotonically decreasing. Thus, with decreasing Fr at given Kn and temperature difference, (1.2) is satisfied only over a diminishing part of the gas layer. Eventually, (1.2) is only satisfied locally at the fluid adjacent to the upper (cold) wall. This occurs at the threshold value

$$Fr_0 = -\frac{4}{5}\left(\frac{\mathrm{d}T^{(0)}}{\mathrm{d}y}\right)^{-1}_{y=1}. \tag{1.3}$$

The above unique attributes of the transition to convection under dominant compressibility effects become more prominent with diminishing Fr which is only slightly larger than Fr_0. We therefore focus on this limit (see (3.1) and (3.2)).

In the next section we formulate the problem. The dispersion relation is subsequently obtained in § 3. In § 4 we present our results for the neutral curve and the corresponding eigenfunctions of the vertical velocity perturbation. We then discuss the non-uniformity of the (generalized) Boussinesq approximation and the analogy between the present limit and the Taylor–Couette (TC) problem. Finally, in § 5 we comment on the relevance of our analysis and point to some desirable extensions. Technical details are relegated to the Appendices.

2. Formulation of the problem

We consider a layer of perfect gas confined between infinite horizontal walls and heated from below. To render the problem dimensionless the gas density is scaled by its average value $\bar{\rho}$ (see (2.6)), the fluid velocity by the mean thermal speed $U_{th} = (2RT_h)^{1/2}$ and the pressure is normalized by $\bar{\rho}RT_h$. Shear viscosity and heat conductivity are normalized by μ_h and κ_h, their respective values at T_h. The dimensionless problem is governed by the continuity equation

$$\frac{\partial \rho}{\partial t} + \nabla\cdot(\rho \boldsymbol{u}) = 0, \tag{2.1}$$

together with the Navier–Stokes

$$\rho\frac{\mathrm{D}\boldsymbol{u}}{\mathrm{D}t}=-\frac{1}{2}\nabla p+Kn\nabla\cdot\left[2\mu\left(\mathbf{e}-\frac{1}{3}\nabla\boldsymbol{u}\right)\right]-\frac{\rho}{Fr}\hat{\boldsymbol{j}} \tag{2.2}$$

and energy

$$\rho\frac{\mathrm{D}T}{\mathrm{D}t}=\frac{\gamma}{Pr}Kn\nabla\cdot(\kappa\nabla T)-(\gamma-1)p\nabla\cdot\boldsymbol{u}+2(\gamma-1)Kn\Phi \tag{2.3}$$

equations as well as the perfect-gas equation of state

$$p=\rho T. \tag{2.4}$$

In the above $\mathrm{D}/\mathrm{D}t$ denotes the material derivative, $\hat{\boldsymbol{j}}$ is a unit vector pointing vertically upwards, $\boldsymbol{u}$ is the velocity vector, and $\mathbf{e}$ and Φ denote the rate-of-strain tensor and the rate of dissipation, respectively. Also appearing in (2.2) and (2.3) are the Knudsen number, $Kn=l/D$ representing the ratio of l, the mean free path, and the macroscopic scale D; the Prandtl number, $Pr=\mu_h c_p/\kappa_h$, and $\gamma=c_p/c_v$, the ratio of specific heats at constant pressure and volume, respectively. For a monatomic hard-sphere gas $\gamma=5/3$, $Pr=2/3$ and the leading-order Chapman–Enskog scheme (Chapman & Cowling 1970) yields for the dimensionless transport coefficients

$$\mu(T)=\kappa(T)=\frac{5\pi^{1/2}}{16}T^{1/2}. \tag{2.5}$$

The above equations are supplemented by the normalization condition

$$\int\rho\,\mathrm{d}V=1, \tag{2.6}$$

specifying the total mass of gas between the walls, and by the boundary conditions

$$v=0,\quad u=\pm\zeta\frac{\partial u}{\partial y},\quad T=\begin{bmatrix}1\\R_T\end{bmatrix}\pm\tau\frac{\partial T}{\partial y}\quad\text{at}\quad y=\begin{bmatrix}0\\1\end{bmatrix}, \tag{2.7}$$

respectively imposing the vanishing of v, the normal velocity component, and specifying the respective magnitudes of u, the tangential-velocity slip, and temperature jump at the lower ($y=0$) and upper ($y=1$) walls. Use of the BGK model yields $\zeta=1.1466Kn$ and $\tau=2.1904Kn$ (Albertoni, Cercignani & Gotusso 1963).

The problem (2.1)–(2.7) possesses the steady 'pure conduction' (i.e. $\boldsymbol{u}^{(0)}=\mathbf{0}$) solution (Stefanov *et al.* 2002)

$$T^{(0)}=(Ay+B)^{2/3},\quad \rho^{(0)}=\frac{C}{T^{(0)}}\exp\left[-\frac{6}{AFr}T^{(0)1/2}\right], \tag{2.8}$$

in which the constants A, B and C are determined by use of (2.6) and (2.7). The linear temporal stability of this reference state is analysed assuming that it is perturbed by small spatially harmonic perturbations. The resulting perturbation problem is transversely symmetric about the y-axis (Manela & Frankel 2005*a*). Thus, without loss of generality, we use a two-dimensional description in the Cartesian coordinates (x, y) whose origin lies on the lower wall and x is a horizontal coordinate axis in

the direction of the wave vector. Accordingly, each of the above-mentioned fields is generically represented by the sum

$$F = F^{(0)}(y) + \phi^{(1)}(y)\exp[\mathrm{i}kx + \omega t] \tag{2.9}$$

wherein $F^{(0)}$ denotes the steady reference state and k is the real wavenumber. Substituting (2.9) into (2.1)–(2.7) and neglecting terms nonlinear in the perturbations we obtain the linear problem consisting of

$$\omega\rho^{(1)} + \frac{\mathrm{d}\rho^{(0)}}{\mathrm{d}y}v^{(1)} + \rho^{(0)}\left[\frac{\mathrm{d}v^{(1)}}{\mathrm{d}y} + f^{(1)}\right] = 0, \tag{2.10}$$

$$\omega\rho^{(0)}f^{(1)} = \frac{1}{2}k^2\left[\rho^{(0)}T^{(1)} + \rho^{(1)}T^{(0)}\right] + Kn\left\{\frac{\mathrm{d}\mu^{(0)}}{\mathrm{d}y}\left[\frac{\mathrm{d}f^{(1)}}{\mathrm{d}y} - k^2v^{(1)}\right] + \mu^{(0)}\left[\frac{\mathrm{d}^2f^{(1)}}{\mathrm{d}y^2} - \frac{k^2}{3}\left(\frac{\mathrm{d}v^{(1)}}{\mathrm{d}y} + 4f^{(1)}\right)\right]\right\}, \tag{2.11}$$

$$\omega\left[\frac{\mathrm{d}\rho^{(0)}}{\mathrm{d}y}f^{(1)} + \rho^{(0)}\frac{\mathrm{d}f^{(1)}}{\mathrm{d}y} + k^2\rho^{(0)}v^{(1)}\right] = Kn\left\{\frac{\mathrm{d}^2\mu^{(0)}}{\mathrm{d}y^2}\left[\frac{\mathrm{d}f^{(1)}}{\mathrm{d}y} - k^2v^{(1)}\right] + 2\frac{\mathrm{d}\mu^{(0)}}{\mathrm{d}y}\left[\frac{\mathrm{d}^2f^{(1)}}{\mathrm{d}y^2} - k^2f^{(1)}\right] + \mu^{(0)}\left[\frac{\mathrm{d}^3f^{(1)}}{\mathrm{d}y^3} + k^2\left(\frac{\mathrm{d}^2v^{(1)}}{\mathrm{d}y^2} - \frac{\mathrm{d}f^{(1)}}{\mathrm{d}y} - k^2v^{(1)}\right)\right]\right\} - \frac{k^2}{Fr}\rho^{(1)}, \tag{2.12}$$

$$\omega\rho^{(0)}T^{(1)} + \rho^{(0)}v^{(1)}\frac{\mathrm{d}T^{(0)}}{\mathrm{d}y} = -\frac{2}{3}\rho^{(0)}T^{(0)}\left[\frac{\mathrm{d}v^{(1)}}{\mathrm{d}y} + f^{(1)}\right] + \frac{5}{2}Kn\left\{\frac{\mathrm{d}\kappa^{(0)}}{\mathrm{d}y}\frac{\mathrm{d}T^{(1)}}{\mathrm{d}y} + \frac{\mathrm{d}T^{(0)}}{\mathrm{d}y}\frac{\mathrm{d}\kappa^{(1)}}{\mathrm{d}y} + \kappa^{(0)}\left[\frac{\mathrm{d}^2T^{(1)}}{\mathrm{d}y^2} - k^2T^{(1)}\right] + \kappa^{(1)}\frac{\mathrm{d}^2T^{(0)}}{\mathrm{d}y^2}\right\} \tag{2.13}$$

wherein $f^{(1)} = \mathrm{i}ku^{(1)}$. These equations are supplemented by the boundary conditions

$$f^{(1)} = \pm\zeta\frac{\mathrm{d}f^{(1)}}{\mathrm{d}y}, \quad v^{(1)} = 0, \quad T^{(1)} = \pm\tau\frac{\mathrm{d}T^{(1)}}{\mathrm{d}y} \tag{2.14}$$

at $y = 0, 1$ respectively. Equation (2.12) was obtained by using both equations of motion to eliminate the pressure term. In (2.11)–(2.13), $\mu^{(0)} = \kappa^{(0)} = (5\pi^{1/2}/16)T^{(0)1/2}$ and $\mu^{(1)} = \kappa^{(1)} = (5\pi^{1/2}/32)T^{(0)-1/2}T^{(1)}$, in accordance with linearization of (2.5). The form (2.9) ensures that $\rho^{(1)}$ satisfies the homogeneous counterpart of (2.6).

3. The dispersion relation

To study the transition to convection under dominant compressibility effects we introduce the small parameter ϵ (see (1.2), (1.3) *et seq.*)

$$Fr = Fr_0(1 + \epsilon), \quad \epsilon \ll 1. \tag{3.1}$$

Inspection of the perturbation problem suggests that the appropriate limit process is defined by the scaling

$$k = l/\epsilon, \quad Kn = a\epsilon^{5/2}, \quad \omega = \sigma\epsilon^{1/2} \tag{3.2}$$

wherein l, a and σ are fixed when $\epsilon \to 0$. Furthermore, (3.2) qualitatively agrees with the above-mentioned earlier observations of Stefanov *et al.* (2002) and Manela & Frankel (2005*a*, *b*). The various perturbation fields are then expanded

$$\left.\begin{aligned} &f^{(1)} \sim \epsilon^{-1}\left(f_0^{(1)} + \epsilon f_1^{(1)} + \cdots\right),\ v^{(1)} \sim v_0^{(1)} + \epsilon v_1^{(1)} + \cdots, \\ &\rho^{(1)} \sim \epsilon^{1/2}\left(\rho_0^{(1)} + \epsilon \rho_1^{(1)} + \cdots\right), \quad T^{(1)} \sim \epsilon^{1/2}\left(T_0^{(1)} + \epsilon T_1^{(1)} + \cdots\right). \end{aligned}\right\} \tag{3.3}$$

For the present limit process the system (2.10)–(2.13) results in a trivial 'outer' (i.e. for $1 - y \sim O(1)$) solution. Seeking an 'inner' matching solution in the vicinity of the upper wall we introduce the coordinate

$$Y = l(1 - y)\epsilon^{-1}, \quad 0 \leqslant Y < \infty, \tag{3.4}$$

and expand the reference state (2.8) about its regular point ($y = 1$, $Fr = Fr_0$)

$$\left.\begin{aligned} &F^{(0)}(y, Fr) \sim F_0^{(0)} + \epsilon F_1^{(0)} + \cdots, \\ &F_0^{(0)} = F^{(0)}(1, Fr_0), \quad F_1^{(0)} = Fr_0\left(\frac{\partial F^{(0)}}{\partial\, Fr}\right)_{(1, Fr_0)} - Y\left(\frac{\partial F^{(0)}}{\partial y}\right)_{(1, Fr_0)}. \end{aligned}\right\} \tag{3.5}$$

Substituting (3.1)–(3.5) into (2.10)–(2.14) we derive in Appendix A the equation

$$\left(\frac{\mathrm{d}^2}{\mathrm{d}\eta^2} - A_0^{-2/7}\right)\left(\frac{\mathrm{d}^2}{\mathrm{d}\eta^2} - A_0^{-2/7} - \Omega\right)\left(\frac{\mathrm{d}^2}{\mathrm{d}\eta^2} - A_0^{-2/7} - \frac{2}{3}\Omega\right)v_0^{(1)} = -\eta v_0^{(1)} \tag{3.6}$$

governing the leading order of the vertical velocity component wherein the new coordinate $\eta = A_0^{1/7}(Y - B_0/A_0)$ is introduced. We further demonstrate in Appendix A that the vanishing at $Fr = Fr_0$ and $y = 1$ of

$$\frac{2}{3}\frac{\mathrm{d}\rho^{(0)}}{\mathrm{d}y}T^{(0)} - \rho^{(0)}\frac{\mathrm{d}T^{(0)}}{\mathrm{d}y}$$

is crucial to the present limit (see § 4 as well). It is this property of the reference state which leads to (3.6) rather than to the standard Boussinesq-type result (Spiegel 1965; Manela & Frankel 2005*b*).

From (2.7) we obtain the boundary conditions

$$\left.\begin{aligned} &v_0^{(1)} = 0, \quad \frac{\mathrm{d}v_0^{(1)}}{\mathrm{d}\eta} = 0, \\ &\left(\frac{\mathrm{d}^2}{\mathrm{d}\eta^2} - A_0^{-2/7}\right)\left(\frac{\mathrm{d}^2}{\mathrm{d}\eta^2} - A_0^{-2/7} - \Omega\right)v_0^{(1)} = 0 \quad \text{at} \quad \eta = -B_0 A_0^{6/7},\ \infty. \end{aligned}\right\} \tag{3.7}$$

At the present level of approximation these respectively reduce to the no-slip and temperature continuity conditions at the upper wall. In (3.6) and (3.7) we denote

$$\left.\begin{aligned} A_0 = \frac{16}{75 l^5 Fr_0^3 a^2 R_T^2}\left(\frac{\rho_0^{(0)}}{\mu_0^{(0)}}\right)^2, \quad B_0 = \frac{8}{15 l^4 Fr_0^2 a^2 R_T}\left(\frac{\rho_0^{(0)}}{\mu_0^{(0)}}\right)^2, \\ \Omega = \frac{l^2\sigma}{A_0^{2/7} a}\frac{\rho_0^{(0)}}{\mu_0^{(0)}}. \end{aligned}\right\} \tag{3.8}$$

The sixth-order ordinary differential operator on the left-hand side of (3.6) is identical to the one appearing within the framework of the Boussinesq approximation. However, the familiar 'Rayleigh term' on the right-hand side of the latter is here replaced by the linearly η-dependent term on the right-hand side of (3.6). This

term changes its sign within the semi-infinite domain of the present problem. It is remarkable that (3.6) is equivalent to the equation governing the azimuthal velocity perturbation in the TC problem for an incompressible viscous fluid within the narrow gap approximation for the case of counter-rotating cylinders (Chandrasekhar 1961; Duty & Reid 1964). We further comment on the analogy between the problems in § 4. Extensive numerical evidence (Manela & Frankel 2005*a*, *b*; see also the beginning of the next section) indicates that the principle of exchange of stabilities is valid throughout the entire domain of parameters of the present RB problem. We therefore focus on the case $\Omega = 0$ where (3.6) and (3.7) respectively reduce to

$$\left(\frac{\mathrm{d}^2}{\mathrm{d}\eta^2} - A_0^{-2/7}\right)^3 v_0^{(1)} = -\eta v_0^{(1)}, \tag{3.9}$$

$$v_0^{(1)}, \quad \frac{\mathrm{d}v_0^{(1)}}{\mathrm{d}\eta}, \quad \left(\frac{\mathrm{d}^2}{\mathrm{d}\eta^2} - A_0^{-2/7}\right)^2 v_0^{(1)} = 0 \quad \text{at} \quad \eta = -B_0 A_0^{6/7}, \infty. \tag{3.10}$$

Similarly to Duty & Reid (1964) the general solution of (3.9) is represented via the superposition

$$v_0^{(1)}(\eta) = \sum_{n=0}^{5} K_n f_n(\eta) \tag{3.11}$$

where K_n $(n = 0, 1, \ldots, 5)$ are arbitrary (complex) constants and

$$f_n(\eta) = \int_{C_n} \exp\left[-\frac{1}{7}z^7 + \frac{3}{5}A_0^{-2/7}z^5 - A_0^{-4/7}z^3 + A_0^{-6/7}z + \eta z\right]\mathrm{d}z \tag{3.12}$$

are generalized Laplace integrals in the complex z-plane. The contours C_n (see figure 3 in Appendix B) originate and terminate at $z \to \infty$ within any of the seven sectors

$$-\frac{\pi}{14} + \frac{2\pi n}{7} < \arg z < \frac{\pi}{14} + \frac{2\pi n}{7} \quad (n = 0, 1, \ldots, 6). \tag{3.13}$$

The requisite dispersion relation is obtained from the six homogeneous algebraic equations for K_n $(n = 0, 1, \ldots, 5)$ resulting from application of the boundary conditions (3.10) at $\eta = -B_0 A_0^{6/7}$ and $\eta = \infty$, respectively. To write the latter, we obtain by use of the method of steepest descents (Appendix B) the leading asymptotic behaviour†

$$f_n(\eta) \approx \sqrt{\frac{\pi}{3}}\eta^{-5/12}\exp\left[\frac{6}{7}\mathrm{e}^{\pi n\mathrm{i}/3}\eta^{7/6} + \frac{3}{5}\mathrm{e}^{-\pi n\mathrm{i}/3}A_0^{-2/7}\eta^{5/6} - \frac{1}{4}\mathrm{e}^{\pi n\mathrm{i}}A_0^{-4/7}\eta^{1/2} + \frac{3}{8}\mathrm{e}^{\pi n\mathrm{i}/3}A_0^{-6/7}\eta^{1/6} - \frac{\pi n\mathrm{i}}{6}\right] \quad \text{at} \quad \eta \to \infty. \tag{3.14}$$

From (3.14) we see that f_2, f_3 and f_4 as well as their respective derivatives become exponentially small as $\eta \to \infty$ whereas f_0, f_1 and f_5 exponentially diverge. Furthermore, no non-trivial combination of the latter may satisfy (3.10) at $\eta \to \infty$, hence K_0, K_1, K_5 necessarily vanish.

To satisfy the remaining boundary conditions (3.10) we numerically compute (3.12) to evaluate $f_n(\eta)$ $(n = 2, 3, 4)$ and their requisite derivatives at $\eta = -B_0 A_0^{6/7}$. Substituting these into (3.10), we obtain a system of three linear homogeneous algebraic

† While Granoff & Bleistein (1972) have systematically studied the asymptotic behaviour of the solutions of (3.9), they have focused on the limit of large wavenumbers for a finite (fixed) η.

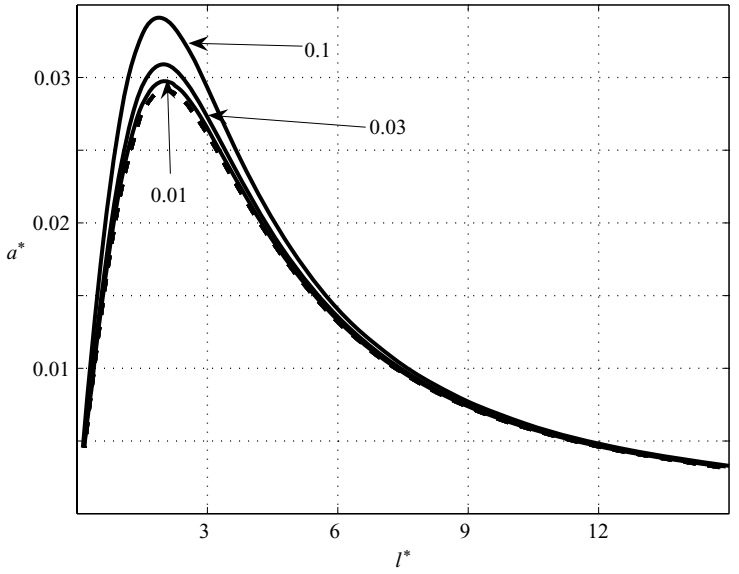

FIGURE 1. The neutral curves in the (l^*, a^*)-plane of generalized wavenumber and Knudsen number for $R_T = 0.5$. The solid lines correspond to the indicated constant values of $\epsilon = Fr/Fr_0 - 1$. The dashed curve depicts the universal dispersion relation (3.15) in the limit $\epsilon \to 0$.

equations for K_2, K_3 and K_4. For this homogeneous system to admit non-trivial solutions we require the vanishing of the characteristic determinant. Taking the lowest branch we obtain the requisite dispersion relation $A_0 = A_0(B_0)$. Hereafter, we present this relation in the form

$$a^* = a^*(l^*) \tag{3.15}$$

wherein

$$l^* = B_0/A_0, \quad a^* = (A_0 l^{*5})^{-1/2} \tag{3.16}$$

are the generalized wavenumber and Knudsen number (see (3.2) and (3.8)). Note that the dispersion relation thus obtained is universal in the sense that it is valid for all $0 < R_T < 1$.

4. Results and discussion

The eigenvalue problem (2.10)–(2.14) has also been solved numerically by means of the Chebyshev collocation method (Peyret 2002). Throughout the entire domain of parameters our calculations yield real-valued growth rates, which supports our focusing in the preceding section on transition to convection through a stationary ($\Omega = 0$) state. In general, for a given temperature ratio R_T, the transition to convection in the compressible RB problem is delineated by a three-dimensional neutral surface in the (Fr, k, Kn) parameter space (Manela & Frankel 2005*a*). Figure 1 presents for $R_T = 0.5$ the neutral curves in the (k, Kn)-plane in terms of l^* and a^* (see (3.2), (3.8) and (3.16)). These curves correspond to constant-Fr (ϵ) sections of the above-mentioned neutral surface in the vicinity of Fr_0. The solid lines result from the numerical calculations at the indicated values of ϵ. The dashed asymptote represents the universal dispersion relation (3.15) in the limit $\epsilon \to 0$. It is nearly indistinguishable from the exact neutral curves for $\epsilon \lesssim 0.01$. We note that with increasing R_T ($\gtrsim 0.7$,

not shown here) the curves approach the (dashed) universal asymptote from below and convergence thereto becomes slower in ϵ.

For all $\epsilon > 0$ and $a^* > 0$ convection is confined to a finite interval of l^* which, with increasing a^*, eventually contracts to a single value l^*_{cr} when $a^* = a^*_{max}(\epsilon)$. With diminishing ϵ, a^*_{max} is approaching the limit $a^*_{max} \approx 0.029$ while the corresponding wavenumber is only slightly increasing to $l^*_{cr} \approx 2$. Recalling that l^*_{cr} and a^*_{max} are respectively related to the wavenumber k_{cr} and the Knudsen number Kn_{max} through the scaling (3.2), the above constant limit $l^*_{cr} \approx 2$ corresponds to a critical wavenumber k_{cr} diverging like $\sim\epsilon^{-1}$ as $\epsilon \to 0$. As already observed by Manela & Frankel (2005*b*), this is in marked contrast to the familiar Boussinesq-type result predicting the constant $k_{cr} \approx 3.117$. Similarly, for a constant a^*_{max}, the corresponding Kn_{max} is diminishing like $\sim\epsilon^{5/2}$ as $\epsilon \to 0$. Thus, for instance, $Kn_{max} \approx 2.6 \times 10^{-4}$ when $\epsilon = 0.1$. This renders DSMC simulations extremely time consuming (Stefanov *et al.* 2002) and therefore rather impractical for the study of the limit $Fr \to Fr_0$.

It seems natural to rescale the critical wavenumber by $\Delta = 1 - y^*$, the normalized width of the gas layer adjacent to the upper wall wherein (1.2) is satisfied. In Δ, y^* denotes the level where the local actual temperature gradient is equal to the adiabatic gradient for a given value of Fr (3.1). From the reference-state temperature distribution (2.8) we obtain

$$\Delta \sim \frac{3R_T^{3/2}}{1 - R_T^{3/2}}[\epsilon + \epsilon^2 + O(Kn)]. \tag{4.1}$$

By use of (3.2), (3.8) and (3.16), the critical wavenumber normalized by Δ is

$$k^*_{cr} = \frac{2\Delta}{5Fr_0 R_T \epsilon} l^*_{cr} \sim l^*_{cr}(1 + \epsilon) \tag{4.2}$$

irrespective of R_T. Hence, when $Fr \to Fr_0$, $k^*_{cr} \to l^*_{cr} \approx 2$. The difference between the present result and the Boussinesq approximation for the critical wavenumber (in fact, for any combination of boundary conditions) is thus not rectifiable merely by an appropriate rescaling.

Figure 2 presents the eigenfunctions (normalized to unity) of the vertical velocity perturbation for $R_T = 0.5$ and the combinations of l^*_{cr} and a^*_{max} at the indicated values of ϵ. The solid lines represent the exact numerical solutions and the dashed lines correspond to the universal asymptote (3.11). For all values of ϵ the figure shows the variation of the eigenfunctions with y, the 'physical' vertical coordinate. This entails duplication of the universal asymptote because of the different 'stretching' imposed by the transformation (3.4) for each ϵ. With diminishing ϵ convection becomes effectively confined to an ever narrowing domain adjacent to the upper (cold) wall. In view of the above this could be anticipated to accompany the diminishing of the interval Δ (4.1) where the necessary condition (1.2) is satisfied. At the indicated values of ϵ, $\Delta \approx 0.09, 0.18$ and 0.29, respectively. The actual corresponding convection domains are roughly twice as wide (cf. Manela & Frankel 2005*a*) owing to viscous momentum diffusion to lower gas layers. Finally, note that despite differences in the respective boundary conditions there is a close similarity between the present eigenfunctions and figure 3 of Duty & Reid (1964) depicting the distribution of the azimuthal velocity perturbation in the TC problem between counter-rotating cylinders (see (3.6)–(3.8) *et seq.*).

The present results concerning the critical wavenumber and the corresponding eigenfunctions hold in the limit $Fr \to Fr_0$ even when the imposed temperature

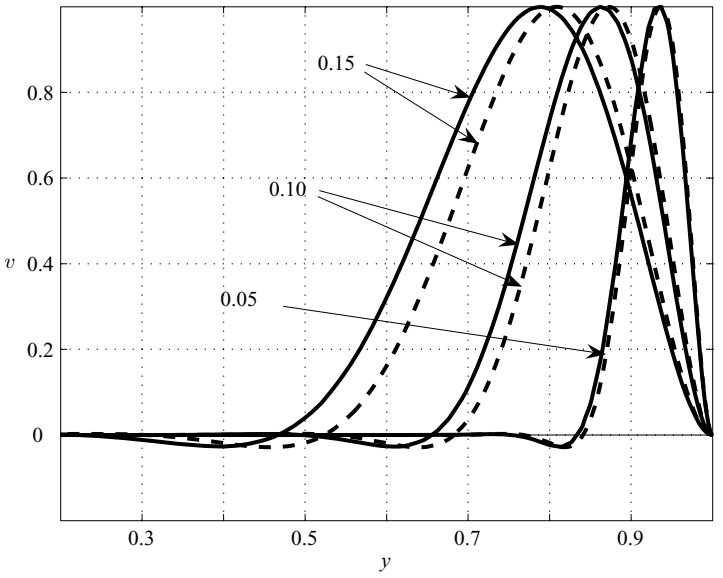

FIGURE 2. The normalized eigenfunctions of the vertical velocity perturbation for $R_T = 0.5$ and the combinations (l^*_{cr}, a^*_{max}) at the indicated values of ϵ (solid lines). The dashed curves represent the universal asymptote (3.11).

difference is small, i.e. $1 - R_T \ll 1$. This seems at odds with the generalized Boussinesq approximation where the actual temperature gradient is replaced by the potential temperature gradient (i.e. the excess over the adiabatic gradient). According to the prevailing view (Tritton 1988), this approximation holds provided that the relative density variations associated with thermal expansion in the reference temperature field and the ratio of the actual vertical scale to the 'scale heights' of the system (over which the various parameters change appreciably) are both small. For a perfect gas the former requirement is equivalent to $1 - R_T \ll 1$ whereas the latter ratio of scales is $O(Fr^{-1})$. Since, from (1.3) and (2.8) (with $Kn \to 0$)

$$Fr_0 = \frac{6R_T^{1/2}}{5\left(1 - R_T^{3/2}\right)} \tag{4.3}$$

both conditions are apparently satisfied. The generalized Boussinesq approximation is therefore non-uniform in the limit $Fr \to Fr_0$. To clarify this we note that in the standard derivation (Jeffreys 1930; Spiegel 1965; Giterman & Steinberg 1970) the variation of heat conductivity with temperature is entirely neglected at the outset. This, in turn, results in a uniform temperature gradient. In the limit $Fr \to Fr_0$ the corresponding potential-temperature gradient uniformly vanishes across the fluid layer and is absent from the dominant balance (see the comments following (3.6) and (A 6)). The generalized Rayleigh number likewise vanishes from the characteristic perturbation equation. This singularity is resolved in the present derivation by considering the (possibly small) variation of the heat conductivity.

While the similarity between the narrow-gap TC problem and the Boussinesq approximation of the RB problem has long been mentioned in the literature (Chandrasekhar 1961) we have here encountered common features between the compressible RB problem and the TC problem between counter-rotating cylinders. Thus, perturbation velocities are governed in both problems by the same equation, (3.6);

the eigenfuctions are similar and the resulting convection is effectively confined to the immediate vicinity of one of the bounding walls.

The above points are related to the qualitative similarities between (1.2) and Rayleigh's condition for the TC problem (Chandrasekhar 1961). Both criteria are obtained via inspection of the resultant force on a fluid element undergoing a virtual displacement satisfying a certain constraint. Thus, in the RB problem we examine whether the adiabatic expansion accompanying a vertical displacement reduces the particle density below that of the ambient fluid. Similarly, in the TC problem we check whether or not a radial displacement at a constant angular momentum results in a restoring centrifugal force on the fluid particle (Rayleigh's criterion). Furthermore, since both derivations do not consider the effects of viscosity they only provide necessary conditions for instability in viscous fluids. Finally, in both cases these necessary conditions are satisfied only within part of the fluid domain: the upper portion of the fluid layer in the RB problem and the domain between the inner cylinder and the nodal surface in the TC problem between counter-rotating cylinders. These domains are monotonically diminishing with increasing compressibility effects or absolute value of the ratio of outer and inner cylinder angular velocities, eventually reducing to vanishingly thin layers adjacent to the upper (cold) wall or the inner cylinder, respectively.

5. Concluding remarks

We have studied the onset of convection in the RB problem under dominant compressibility effects, i.e. in the limit $Fr \to Fr_0$. Unlike the familiar Boussinesq approximation, transition to convection is characterized in this limit by large (diverging) critical wavenumbers and the resulting convection is confined to a narrow domain adjacent to the upper (cold) wall. Similar features appear in the final (steady-state) convection patterns presented by Stefanov *et al.* (2002) for diminishing Kn and Fr on the neutral curve (see their figures 2 and 3). These patterns were obtained via simulations of system evolution in the corresponding fully nonlinear initial-value problem. As such, they support the relevance of the present linear analysis to the actual onset of convection at slightly super-adiabatic conditions which may prevail in large-scale geophysical systems (Tritton 1988).

Explicit results have been presented for a hard-sphere gas (which could readily be extended to other models of molecular interaction, cf. Manela & Frankel 2005*b*) and temperature ratio $R_T = 0.5$. Similar agreement between numerical and asymptotic results as presented in figures 1 and 2 has been obtained for other values of R_T including cases where $1 - R_T \ll 1$ (i.e. small temperature differences) as well. This indicates that the generalized Boussinesq approximation is non-uniform in the limit $Fr \to Fr_0$. This singularity is resolved in the present analysis by considering the (commonly neglected) effect of the variation of fluid properties which becomes significant in the present limit owing to the apparent vanishing from the dominant balance of the potential-temperature gradient.

In conclusion we note that, while (1.2) is usually irrelevant under conditions that may be realized in laboratory experiments, it may become dominant in the onset of convection in near-critical fluids owing to the rapid increase of the coefficients of compressibility and thermal expansion when approaching the gas–liquid critical point. This has indeed been verified experimentally (e.g. Ashkenazi & Steinberg 1999; Kogan & Meyer 2001). The experimental results are commonly interpreted in terms of the generalized Boussinesq approximation (Carlés & Ugurtas 1999) neglecting fluid stratification. Carlés & Ugurtas (1999), however, point out that their

assumption of uniform fluid properties may cease to apply close to the gas–liquid critical point. Furthermore, Kogan & Meyer (2001) report on increasing difficulty in unambiguously determining the temperature difference requisite for the onset of convection when approaching the critical point. This is manifested in the 'transition rounding' in their figure 2(c, d). Kogan & Meyer suggest that this phenomenon may be related to some technical problems (e.g. temperature-control quality) arising from growing sensitivity of their experimental setup. Increasing the overall temperature difference by increasing T_h (as done in Kogan & Meyer's experiment) corresponds in the present analysis to a growing Fr/Fr_0. The gradual widening of the convection domain within the cell, as predicted by our calculations when Fr/Fr_0 exceeds unity, may thus serve to rationalize Kogan & Meyer's observations. Evidently, a near-critical fluid does not obey the perfect-gas equation of state. It thus seems desirable to extend the present analysis to incorporate constitutive relations of broader generality.

Appendix A. Derivation of (3.6)

Substituting (3.1)–(3.5) into (2.10)–(2.12) we obtain for the respective leading orders of the continuity ($O(\epsilon^{-1})$) and momentum ($O(\epsilon^{-3/2})$) equations

$$-l\frac{\mathrm{d}v_0^{(1)}}{\mathrm{d}Y}+f_0^{(1)}=0, \tag{A 1}$$

$$\rho_0^{(1)}+\frac{\rho_0^{(0)}}{T_0^{(0)}}T_0^{(1)}=0, \tag{A 2}$$

$$\sigma\rho_0^{(0)}\left[-\frac{\mathrm{d}^2v_0^{(1)}}{\mathrm{d}Y^2}+v_0^{(1)}\right]=al^2\mu_0^{(0)}\left[-\frac{\mathrm{d}^4v_0^{(1)}}{\mathrm{d}Y^4}+2\frac{\mathrm{d}^2v_0^{(1)}}{\mathrm{d}Y^2}-v_0^{(1)}\right]-\frac{1}{Fr_0}\rho_0^{(1)}. \tag{A 3}$$

The $O(\epsilon^{-1})$ leading order of the energy equation (2.13) is identical to (A 1). To obtain the $O(1)$ and $O(\epsilon)$ corrections of (2.13) we need the same orders of (2.10). These are, respectively,

$$-l\frac{\mathrm{d}v_1^{(1)}}{\mathrm{d}Y}+f_1^{(1)}=-\frac{\rho_0^{(0)\prime}}{\rho_0^{(0)}}v_0^{(1)} \tag{A 4}$$

and

$$-l\frac{\mathrm{d}v_2^{(1)}}{\mathrm{d}Y}+f_2^{(1)}=-\frac{\rho_0^{(0)\prime}}{\rho_0^{(0)}}v_1^{(1)}+\left[-\frac{\rho_1^{(0)\prime}}{\rho_0^{(0)}}+\frac{\rho_1^{(0)}\rho_0^{(0)\prime}}{\rho_0^{(0)2}}\right]v_0^{(1)}-\sigma\frac{1}{\rho_0^{(0)}}\rho_0^{(1)} \tag{A 5}$$

wherein a prime denotes y-derivatives of the reference 'pure conduction' state. From (A 1) and (A 4) we find that the $O(1)$ correction of (2.13),

$$\left[-\rho_0^{(0)}T_0^{(0)\prime}+\tfrac{2}{3}\rho_0^{(0)\prime}T_0^{(0)}\right]v_0^{(1)}=0, \tag{A 6}$$

is trivially satisfied owing to the vanishing of the expression in brackets. From (A 1), (A 2) and (A 4)–(A 6) we obtain for the next ($O(\epsilon)$) correction of the energy equation

$$\frac{5}{3}\sigma\rho_0^{(0)}T_0^{(1)}=\left[\rho_1^{(0)}T_0^{(0)\prime}-\rho_0^{(0)}T_1^{(0)\prime}+\frac{2}{3}\left(\rho_0^{(0)\prime}T_1^{(0)}+T_0^{(0)}\rho_1^{(0)\prime}\right)\right]v_0^{(1)}+\frac{5}{2}al^2\kappa_0^{(0)}\left[\frac{\mathrm{d}^2T_0^{(1)}}{\mathrm{d}Y^2}-T_0^{(1)}\right]. \tag{A 7}$$

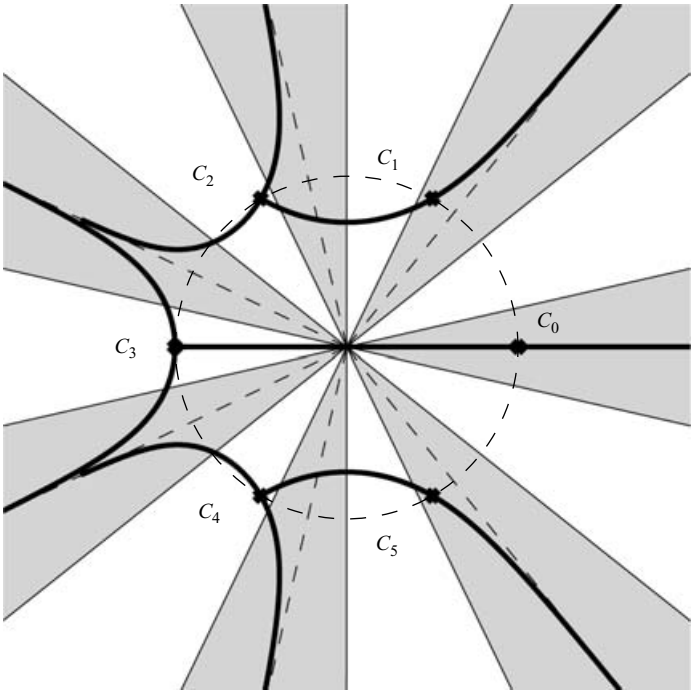

FIGURE 3. The steepest-descent contours (solid lines), passing through the saddle points (crosses), used to obtain the asymptotic estimate (3.14) as $\eta \to \infty$. The shaded areas mark the sectors (3.13). The contours are asymptotic to the dashed rays bisecting the shaded zones. When $\lambda \to \infty$ the saddle points are located on the dashed circle whose radius is $A_0^{-1/7}$.

Finally, eliminating $T_0^{(1)}$ and $\rho_0^{(1)}$ by use of (A 2) and (A 3), (A 7) readily yields (3.6) for $v_0^{(1)}$. The corresponding boundary conditions (3.7) are similarly obtained.

It has been verified that higher-order corrections of the continuity ($O(\epsilon^{n+2})$), momentum ($O(\epsilon^{n-1/2})$) and energy ($O(\epsilon^{n+2})$) equations result in consistent systems of equations governing $\rho_{n+1}^{(1)}$, $f_{n+1}^{(1)}$, $v_{n+1}^{(1)}$ and $T_{n+1}^{(1)}$ for $n = 0, 1, \ldots,$ respectively.

Appendix B. Approximation of f_n at $\eta \to \infty$

To apply the method of steepest descents (Murray 1974) to the approximation of $f_n(\eta)$ as $\eta \to \infty$ we introduce the transformation

$$\eta = \lambda^6, \quad z = \lambda p, \quad \lambda \to \infty \tag{B 1}$$

to obtain from (3.12)

$$f_n(\lambda) = \lambda \int_{C_n} \exp[\lambda^7 h(p;\lambda)]\, \mathrm{d}p \tag{B 2}$$

wherein

$$h(p;\lambda) = -\tfrac{1}{7}p^7 + p + g(p;\lambda), \quad g(p;\lambda) = \tfrac{3}{5}\gamma^2 p^5 - \gamma^4 p^3 + \gamma^6 p \tag{B 3}$$

and $\gamma = (-A_0)^{-1/7}\lambda^{-1} \to 0$. The saddle points of h, satisfying $\mathrm{d}h/\mathrm{d}p = 0$, are

$$p_n = \pm[\exp(2\pi n/3)\mathrm{i} + \gamma^2]^{1/2}, \quad n = 0, 1, 2. \tag{B 4}$$

The constant-phase contours passing through these points (steepest descent and steepest ascent contours) thus satisfy

$$\psi_n = \mathrm{Im}\{h\} = \mathrm{Im}\{h(p_n)\}. \tag{B 5}$$

Figure 3 presents the contours of steepest descents (solid lines) passing through each of the saddle points (crosses) obtained from (B 4) and (B 5) in the limit $\lambda \to \infty$ ($\gamma \to 0$). Also presented (shaded zones) are the sectors (3.13) where these contours originate and terminate. (The figure is similar to figure 4 in Granoff & Bleistein 1972 and is presented here for easy reference.) Making use of (B 3) and (B 4) we obtain for the leading order of (B 2)

$$f_n \approx \sqrt{\frac{\pi}{3}}\lambda^{-5/2}\exp[\lambda^7 h(p_n) - \pi n\mathrm{i}/6] \tag{B 6}$$

which, when written explicitly, yields (3.14).

In conclusion of this Appendix, the following comments are appropriate. We first note that Duty & Reid (1964) were similarly concerned with the asymptotic behaviour of the solutions of (3.9) when $\eta \to \infty$. In the present notation they expanded their solution in powers of $\lambda^7 g$. While the resulting series is convergent for all finite $\lambda^7 g$ (the integrand of (B 2) being holomorphic), it is readily verified that it does not yield an asymptotic series for $\eta \to \infty$.

Finally, we observe that, owing to the dependence of $h(p;\lambda)$ upon λ, (B 2) is not strictly a Laplace integral. The standard steepest descent scheme is nevertheless applicable since $h(p;\lambda)$ is analytic for $\lambda \to \infty$. Consequently, the corresponding picture of saddle points and steepest-descent contours is uniformly convergent in this limit.

REFERENCES

Albertoni, S., Cercignani, C. & Gotusso, L. 1963 Numerical evaluation of the slip coefficient. *Phys. Fluids* **6**, 993–996.

Ashkenazi, S. & Steinberg, V. 1999 High Rayleigh number turbulent convection near the gas-liquid critical point. *Phys. Rev. Lett.* **83**, 3641–3644.

Bormann, A. 2001 The onset of convection in Rayleigh-Bénard problem for compressible fluids. *Continuum Mech. Thermodyn.* **13**, 9–23.

Carlés, P. & Ugurtas, B. 1999 The onset of free convection near the liquid-vapour critical point-part I: Stationary initial state. *Physica D* **126**, 69–82.

Chandrasekhar, S. 1961 *Hydrodynamic and Hydromagnetic Stability*. Clarendon.

Chapman, S. & Cowling, T. 1970 *The Mathematical Theory of Non-Uniform Gases*, 3rd edn. Cambridge University Press.

Duty, R. L. & Reid, W. H. 1964 On the stability of viscous flow between rotating cylinders. *J. Fluid Mech.* **20**, 81–94.

Frölich, J., Laure, P. & Peyret, R. 1992 Large departures from Boussinesq approximation in the Rayleigh-Bénard problem. *Phys. Fluids* A **4**, 1355–1372.

Giterman, M. & Shteinberg, V. 1970 Criteria of occurrence of free convection in a compressible viscous heat-conducting fluid. *J. Appl. Maths Mech.* **34**, 325–331.

Golshtein, E. & Elperin, T. 1996 Convective instabilities in rarefied gases by direct simulation Monte Carlo method. *J. Thermophys. Heat Transfer* **10**, 250–256.

Granoff, B. & Bleistein, N. 1972 Asymptotic solutions of a 6th order differential equation with two turning points. Part 1: Derivation by method of steepest descent. *SIAM J. Math. Anal.* **3**, 45–57.

Jeffreys, H. 1930 The instability of compressible fluid heated below. *Proc. Camb. Phil. Soc.* **26**, 170–172.

Kogan, A. B. & Meyer, H. 2001 Heat transfer and convection onset in a compressible fluid: ^{3}He near the critical point. *Phys. Rev.* E **63**, 056310.

Koschmieder, E. 1993 *Bénard Cells and Taylor Vortices*. Cambridge University Press.

Landau, L. & Lifshitz, E. 1959 *Fluid Mechanics*. Pergamon.

Manela, A. & Frankel, I. 2005*a* On the Rayleigh-Bénard problem in the continuum limit. *Phys. Fluids* **17**, 036101.

Manela, A. & Frankel, I. 2005*b* On the Rayleigh-Bénard problem in the continuum limit: Effects of temperature differences and model of interaction. *Phys. Fluids* **17**, 118105

Murray, J. D. 1974 *Asymptotic Analysis*. Clarendon.

Paolucci, S. & Chenoweth, D. R. 1987 Departures from the Boussinesq approximation in the laminar Bénard convection. *Phys. Fluids* **30**, 1561–1564.

Peyret, R. 2002 *Spectral Methods for Incompressible Viscous Flow*. Springer.

Sone, Y., Aoki, K. & Sugimoto, S. 1997 The Bénard problem for a rarefied gas: Formation of steady flow patterns and stability of array of rolls. *Phys. Fluids* **9**, 3898–3914.

Spiegel, E. A. 1965 Convective instability in a compressible atmosphere. I. *Astrophys. J.* **141**, 1068–1089.

Stefanov, S. & Cercignani, C. 1992 Monte Carlo simulation of Bénard's instability in a rarefied gas. *Eur. J. Mech.* B/*Fluids* **11**, 543–554.

Stefanov, S., Roussinov, V. & Cercignani, C. 2002 Rayleigh-Bénard flow of a rarefied gas and its attractors. I. Convection regime. *Phys. Fluids* **14**, 2255–2269.

Tritton, D. J. 1988 *Physical Fluid Dynamics*. Clarendon.